Paper No.
19145

AMPP ANNUAL CONFERENCE + EXPO
MARCH 19-23, 2023 | DENVER, COLORADO

Adsorption of Model Inhibitor Compound Characterized Using Quartz Crystal Microbalance with Dissipation Monitoring

Kushal Singla [a], Hubert Perrot [b], Bruce Brown [a], Srdjan Nesic [a]

[a]Institute for Corrosion and Multiphase Technology (ICMT), Department of Chemical & Biomolecular Engineering, Ohio University, Athens, OH 45701

[b]Sorbonne Université, CNRS, Laboratoire Interfaces et Systèmes Electrochimiques (LISE, UMR 8235), 4, place Jussieu, (case courrier 133), F-75005, Paris, France

ABSTRACT

Although inhibitor adsorption and inhibition mechanisms have been studied extensively using various electrochemical techniques, these electrochemical techniques only provide an indirect estimate of inhibitor adsorption. In the present study, a QCM with dissipation monitoring (QCM-D) was used to investigate the adsorption on gold coated quartz crystal resonator (QCR) of a model corrosion inhibitor (CI) compound at different bulk inhibitor concentrations. In a first step, the classical Sauerbrey's equation was used to analyze the normalized frequency change data for estimation of adsorbed mass. Normalized frequency change was also analyzed in conjunction with dissipation change using small load approximation (SLA) model to establish the nature of adsorbed layer and to qualify the validity of Sauerbrey's equation. In context of the bulk inhibitor concentrations tested (50 ppm(w) and 100 ppm(w) of CI in 1wt.% NaCl solution) in this study, the adsorbed layer behaves as a rigid mass. A conscious effort is made to state and validate the assumptions for the analysis of experimental results.

Keywords: Corrosion inhibitor, inhibitor adsorption, inhibition, Sauerbrey equation, QCM, QCM-D

INTRODUCTION

Oil and gas transportation pipelines are often prone to internal corrosion in service environments. Two main strategies used to combat the problem of internal corrosion in pipelines involve the use of corrosion inhibitors (CIs) and more corrosion resistant alloys. Corrosion mitigation using inhibitors is a favorable choice because of better economic feasibility.[1–4] Among all the types of corrosion inhibitors, organic corrosion inhibitors are most widely used in the industry.

Organic corrosion inhibitors are typically surfactant-type organic molecules with a hydrophilic head group and a hydrophobic alkyl tail. Corrosion inhibition using organic CIs relies on the mechanisms related to the adsorption of inhibitor molecules on a metal surface.[2,4] However, the exact adsorption mechanisms are not yet clearly understood. So, in designing CIs with improved efficiency and to have a better understanding of underlying inhibition mechanisms, it becomes extremely important to study and quantify

adsorption mechanisms. Various studies focusing on electrochemical experiments have been performed in the past but due to the intrinsic limitations of traditional electrochemical techniques, there is a lack of molecular level understanding of electrode/electrolyte interfacial properties such as adsorbed layer thickness, orientation of adsorbed inhibitor molecules etc. in the presence of corrosion inhibitor.[5–7]

Adsorption of CIs is a surface phenomenon happening at the electrode/electrolyte interface. Quartz crystal microbalance (QCM) is a powerful surface acoustic sensor that can be effectively used to study surface reactivity.[8] With recent advances in technology, a QCM-D (QCM with dissipation monitoring and measurements at multiple overtones) can now be used to delve into the territory of characterizing the mechanical properties of the adsorbed layer.[9] QCM-D as a tool has found an extensive application in the field of protein adsorption but has been minimally applied in corrosion inhibition research. This project makes a conscious effort to borrow the learnings from a different field of science, learn, understand, and develop a tool for corrosion related research.

With this motivation, a QCM-D equipped with a flow control unit was used for better understanding of an electrode/electrolyte interface to understand the nature of the adsorbed layer and quantify the adsorbed layer thickness for a model inhibitor compound, tetradecyldimethylbenzylammonium (BDA-C14), on a noble substrate (gold for QCM-D) in 1 wt.% NaCl solution. In this paper, adsorption experiments are discussed for BDA-C14 at two inhibitor concentrations (50 ppm(w) and 100 ppm(w)). Based on the frequency change and dissipation change vs. time, experimental results are discussed for qualitative indications and quantitative analysis primarily for the adsorbed layer thickness.

EXPERIMENTAL PROCEDURE

Model corrosion inhibitors such as quaternary ammonium-based compounds and imidazolines with different alkyl tail lengths have been synthesized in-house for multiple research projects at the ICMT.[10–12] The rationale of using lab synthesized model compounds was to decrease the number of unknowns in the experiments because it is understood that commercial CI packages contain certain formulations which are trade secrets.[1,2] For this study, the adsorption behavior of BDA-C14 has been tested since it has already been well characterized.[10–12] BDA-C14 is a quaternary ammonium type model inhibitor compound with alkyl tail having fourteen carbons as shown in Figure 1. Test conditions for this experiment are presented in Table 1.

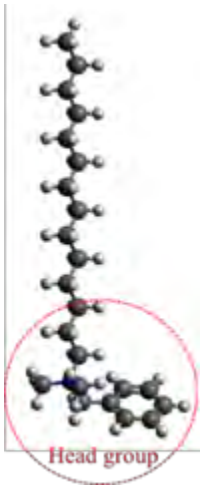

Figure 1: BDA-C14; a quaternary ammonium-type corrosion inhibitor.[13]

Table 1: Test matrix for inhibitor adsorption on gold coated QCR.

Parameter	Value
Base Electrolyte	1 wt. % NaCl in deionized water
Inhibitor Solution	50 ppm(w) & 100 ppm(w) BDA-C14 in base electrolyte
Substrate/QCR	5 MHz, wrapped around configuration[12], Au/Ti, polished
Operating overtones	n=1, 3, 5, 7, 9, 11 and 13
Flow rate	0.05 mL/minute

The QCM-D unit used for this study monitors frequency change and dissipation change at multiple overtones simultaneously (n=1, 3, 5, 7, 9, 11 and 13).[14,15] AT-cut gold coated, polished quartz crystals with a fundamental resonance frequency of ~5 MHz were used as the substrates.[§] Figure 2 shows the QCM-D experimental setup that was used for inhibitor adsorption experiments. Firstly, base electrolyte solution (base solution) without any inhibitor was pumped through the QCM unit cell at a constant flow rate to get a baseline frequency response against which any change in frequency due to mass adsorption was measured. Then, the valve at the syringe pump was switched to flow inhibitor solution (CI solution) through the QCM cell while the change in frequency and dissipation values were measured with respect to time. Experimental data is represented in terms of frequency change and dissipation change with respect to time.

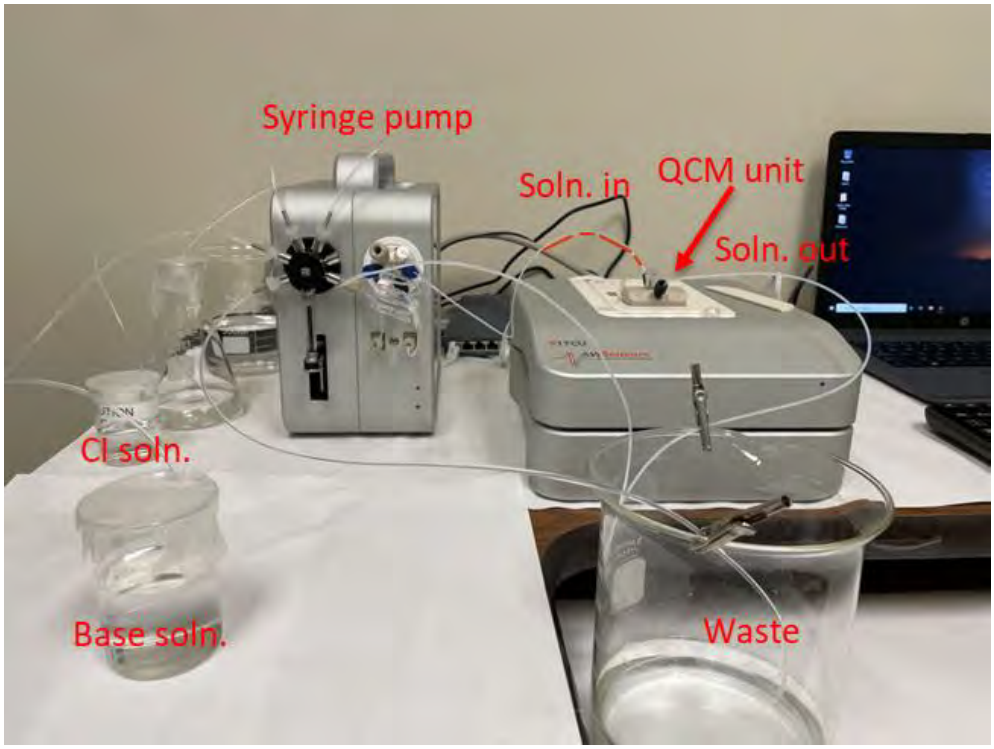

Figure 2: QCM-D setup with flow control unit used for inhibitor (BDA-C14) adsorption.

[§] purchased from Advanced Wave Sensors S.L., (Paterna, Spain).

METHODOLOGY

Recorded frequency change and dissipation change can be analyzed in two ways:

1. Qualitative indications: Based on certain signatures in frequency and dissipation change data recorded with respect to time, some preliminary predictions can be made about the nature of adsorbed mass (rigid or viscoelastic). Figure 3 suggests that:

a) For no mass deposit, there is no change observed with respect to time for normalized frequency change and dissipation change. This is often referred to as baseline in QCM experiments. Obtaining a stable baseline is equally important in any QCM based measurements as any change due to an adsorption/desorption process is measured with respect to a stable baseline.
b) For a rigid mass deposit, dissipation change with respect to time is small or negligible and there is no split in dissipation change values at multiple overtones. Net frequency change for such cases can be used directly for estimation of adsorbed mass using Sauerbrey's equation.
c) For a viscoelastic mass, dissipation change with respect to time cannot be neglected anymore and hence should be part of any quantitative analysis. The validity of Sauerbrey's equation would no longer hold for calculation of net adsorbed mass at the surface of the QCR. In addition to net dissipation change, there is also an obvious split observed in the frequency change and dissipation change values measured at different overtones which can be related to the mechanical properties of adsorbed layer. Consideration of the magnitude of dissipation is necessary to make any conclusions.

2. Quantitative analysis: To estimate the adsorbed layer thickness and mechanical properties of the adsorbed layer, different models can be used to analyze QCM-D data such as Sauerbrey's model (applicable for rigid films only), small load approximation (SLA) model, and Voigt based viscoelastic model.[8,16–18] For the results analyzed in this paper, Sauerbrey's model and SLA model were used.

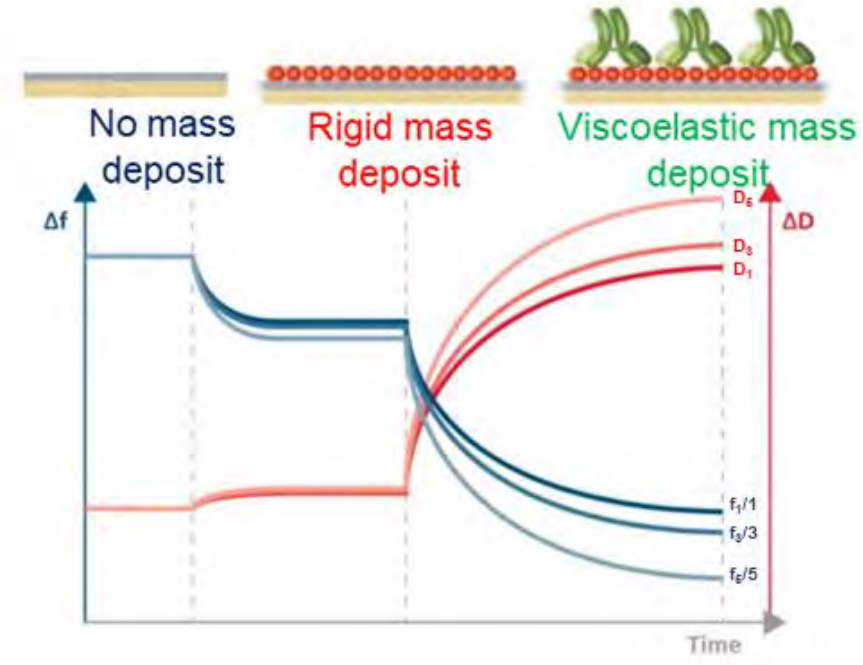

Figure 3: Schematic of frequency and dissipation response using QCM-D at multiple harmonics for rigid and viscoelastic mass deposit.[9]

RESULTS AND DISCUSSION

The aim of the experiments was to investigate inhibitor adsorption via measuring a change in resonance frequency and dissipation values using the QCM-D equipped with a flow control unit. Any decrease in frequency refers to adsorption because when mass gets adsorbed on QCR, the resonance frequency decreases.[8,12,16] Figure 4 and Figure 5 show the normalized frequency change (left y-axis) and dissipation change (right y-axis) measured with respect to time (x-axis) at multiple overtones (n = 7, 9 and 11) for inhibitor concentrations of 50 ppm(w) and 100 ppm(w) respectively.

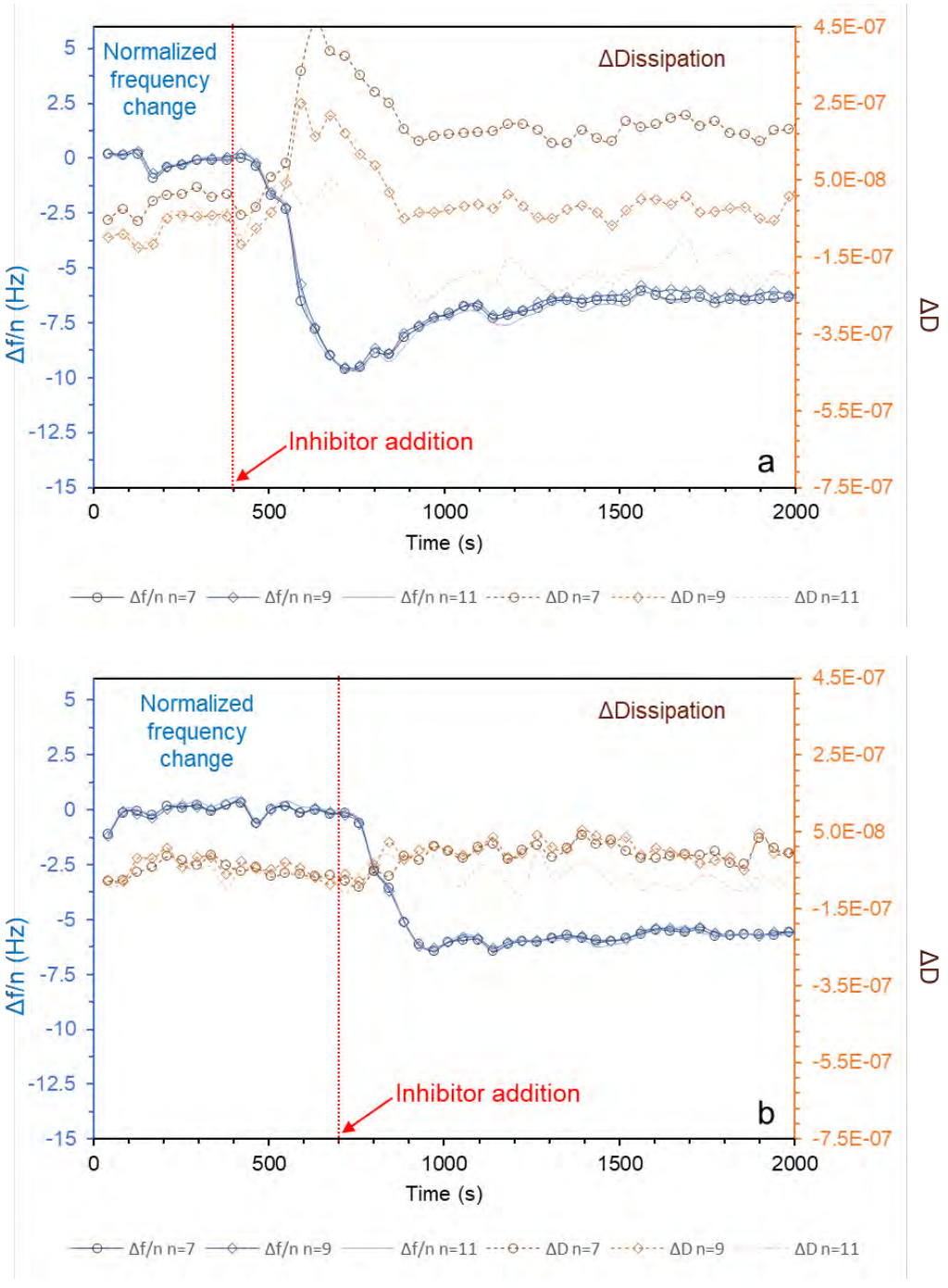

Figure 4: Normalized frequency change (in blue shades) and dissipation change (in orange shades) vs. time for inhibitor concentration of 50 ppm(w). (a) and (b) are results of two separate experiments.

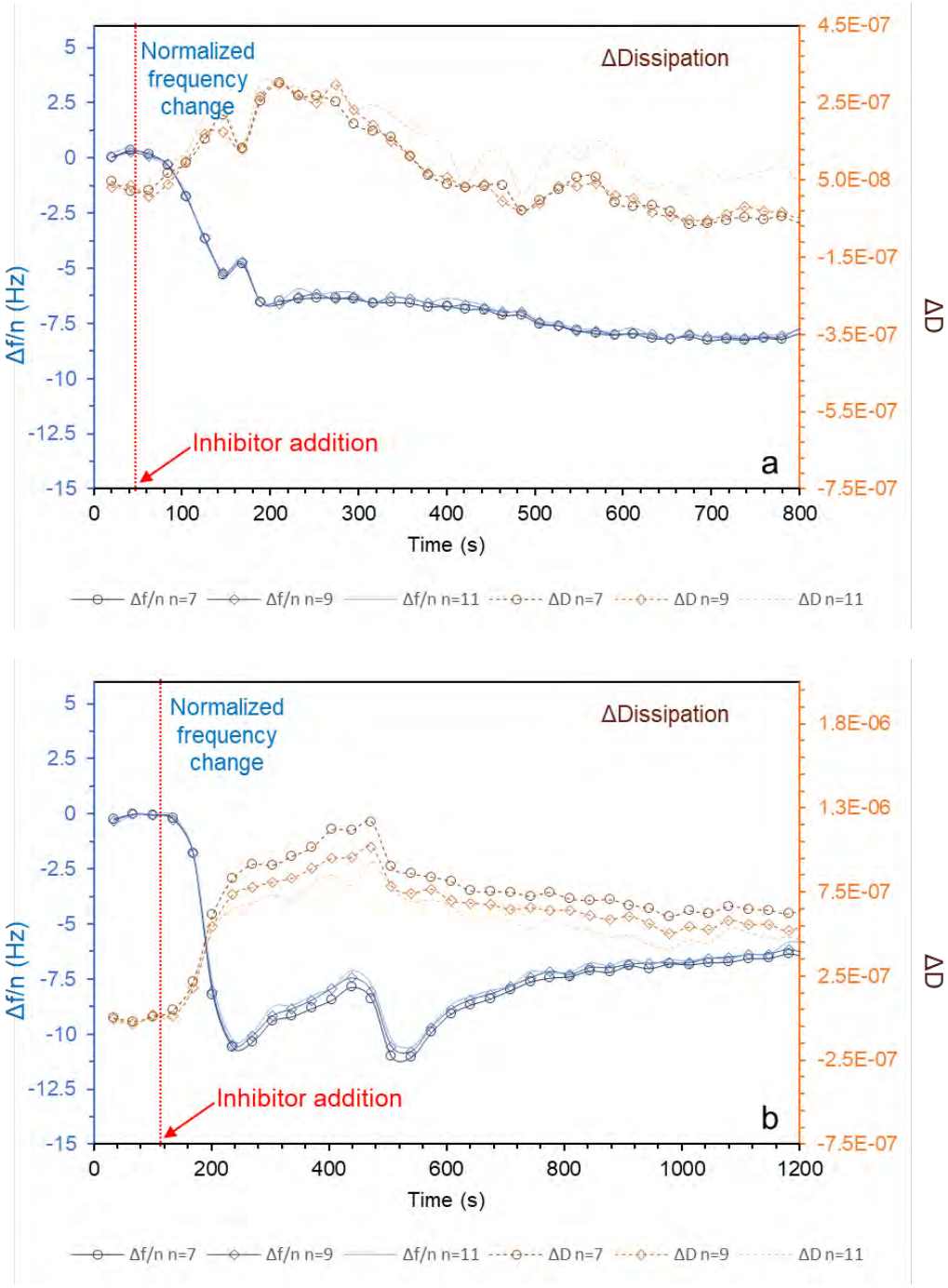

Figure 5: Normalized frequency change (in blue shades) and dissipation change (in orange shades) vs. time for inhibitor concentration of 100 ppm(w). (a) and (b) are results of two experiments.

Qualitative Indications

For all the experiments, a clear baseline in frequency was observed at multiple overtones and it was also observed that the adsorption step was fast and happened within a few minutes. After the adsorption step, the split in dissipation values is observed at multiple overtones in Figure 4a which indicates a viscoelastic mass deposit. But this split in dissipation values was not consistent for all the experiments as it is not observed in Figure 4b and Figure 5a. So, to summarize, nothing can be concluded convincingly about the nature of adsorbed mass from Figure 4 and Figure 5. However, notice that the value of dissipation

change for these inhibitor adsorption experiments is 10^{-8} - 10^{-7}. It has been reported in literature that a viscoelastic mass adsorption, such as proteins or cell adsorption, typically influences the change in dissipation (ΔD) on the order of 10^{-4} - 10^{-5}.[9] With a dissipation change in these inhibitor adsorption experiments measured to be orders of magnitude lower than reported values typical for a viscoelastic mass, it can be reasonably inferred that the absorbed inhibitor layer behaves as a rigid mass. This is an assumption based on comparison with reported literature and needs to be validated in further data analysis. Later in this document, absorbed layer properties are estimated using the SLA model in quantitative analysis, which will shed more light on the validity of a rigid mass assumption. For now, since it is inferred that adsorbed mass is rigid in nature, Sauerbrey's equation can be used to estimate the adsorbed mass per unit area.[8,16] Table 2 summarizes the adsorbed mass per unit area calculated using Sauerbrey's equation.

$$\frac{\Delta m_{QCM}}{A} = -\left(\frac{\left(\frac{\Delta f_{mass}}{n}\right)}{C_f}\right) \quad (1)$$

where,

$$C_f = -2f_o^2\left(\mu_q\rho_q\right)^{-\frac{1}{2}} \quad (2)$$

Δf_{mass} - change in resonance frequency measured using QCM, Hz
n - number of overtones
A - piezoelectrically active area, cm^2 (area of overlap between two electrodes)
f_o - fundamental resonance frequency of QCR, Hz
μ_q - shear modulus for quartz crystal (2.947 x 10^{11} $g \cdot cm^{-1} \cdot s^{-2}$)
ρ_q - density of quartz crystal (2.648 $g \cdot cm^3$)

✓ In air, theoretical value of C_f for 5 MHz AT-cut quartz crystal is 56.6 $Hz \cdot \mu g^{-1} \cdot cm^2$

Table 2: Results summary for inhibitor adsorption experiments.

Parameter	Average value	
	50 ppm(w)	**100 ppm(w)**
Δf (Hz)	6.4 ± 0.3	7.9 ± 0.9
$\Delta m_{QCM}/A$ ($ng \cdot cm^{-2}$)	113 ± 5	139 ± 15.9

Quantitative Analysis

For quantitative analysis of QCM-D data, a QTM software tool[**] based on the SLA model was used. The mathematical approach for this model is based on solving the wave equation assuming continuity of displacement and stress for various interfaces such as electrode/adsorbed mass interface or adsorbed mass/ bulk solution interface.[17,19,20] The software tool fits the measured normalized frequency change and dissipation change by using different fitting parameters such as, density of the adsorbed layer, complex shear stress (G'/G''),or viscoelastic compliance (J'/J''). Based on the fitting quality and physical significance of obtained parameters, apparent averaged adsorbed layer thickness can be obtained as a function of time. It is important to mention here that QCM-D measures average mass added on surface but analysis using the SLA model gives apparent average thickness as an output. The conversion

[**] Advanced Wave Sensors S.L., (Paterna, Spain).

between surface mass adsorbed and apparent average thickness can be done assuming adsorbed layer density of 1 g·cm^{-3} for bulk aqueous solutions.[17,19,20] Figure 6 shows one example of fitting exercise for 50 ppm(w) inhibitor concentration and Figure 7 shows the corresponding adsorbed mass per unit area (original data corresponds to Figure 4a).

For this analysis:

i. Experimental data: Δf/n and ΔD, referred as Df/n and DD in Figure 6 respectively
ii. Fitting parameters: viscoelastic compliance, J'/J''
iii. Input parameters: adsorbed layer density (1 g·cm^{-3})
iv. Output: space averaged adsorbed layer thickness (nm)

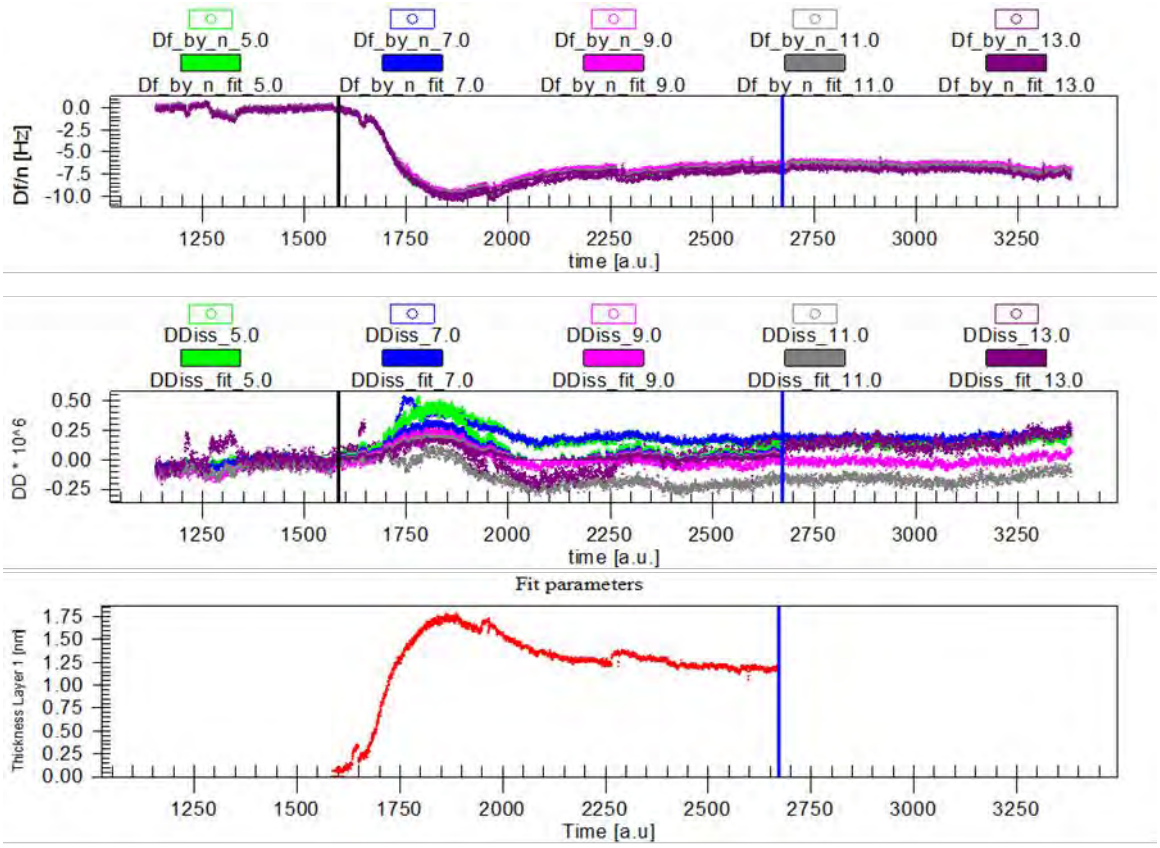

Figure 6: Example of data fitting using QTM tool, 50 ppm(w) bulk inhibitor concentration, time axis is in seconds (s) scale and data corresponds to Figure 4a.

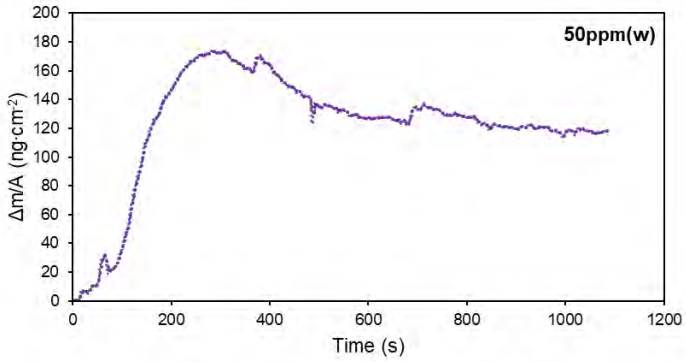

Figure 7: Mass adsorbed per unit area, converted from apparent average thickness estimated using QTM tool, 50 ppm(w) bulk inhibitor concentration, data corresponds to Figure 4a.

This fitting exercise was repeated for all the experiments and Table 3 shows the results obtained for the equilibrium adsorbed layer thickness at two inhibitor concentrations. It should be noted here that the input value for the adsorbed layer density was defined as 1 g·cm^3 which needs to be validated. This was done for the reason that a QCM always measures an areal density, never a geometric thickness. Hence, thickness calculations require an independent input of physical density. The validity of this assumption is tested and discussed later in the document.

Compliance, which can be thought of as the inverse of modulus, (elastic compliance J'/ viscous compliance J'') was used as a fitting parameter to calculate the adsorbed layer thickness. As a result of QTM tool fitting, values obtained for J' and J'' are ~10^{-1} MPa^{-1} and ~10^{-5} MPa^{-1} respectively. This suggests that the adsorbed layer is elastic (rigid) in nature. More precisely, the adsorbed layer behaves as a rigid mass when compared with the ambient bulk liquid. This result is aligned well with the initial inference based on qualitative analysis and validates the use of Sauerbrey's equation. The adsorbed mass per unit area estimated using Sauerbrey's equation and SLA model (assuming an adsorbed layer density of 1 g·cm^{-3}) are considered the same when taking into account the measurement error (Table 3), which further validates the rigid mass assumption.

Table 3: Summary of QCM-D results.

Methodology	Parameter	Average value	
		50 ppm(w)	100 ppm(w)
By fitting of Δf/n and ΔD using SLA model	*Adsorbed layer thickness (nm)*	1.17 ± 0.06	1.53 ± 0.08
Adsorbed mass based on SLA model and using density of 1 g·cm^{-3}	Δm/A (ng·cm^2)	117 ± 6	153 ± 8
From Sauerbrey's equation calculation	Δm/A (ng·cm^2)	113 ± 5	139 ± 15.9

In a separate study conducted using atomic force microscopy (AFM) by Wang et al., the absorbed layer thickness for BDA-C14 at 100 ppm(w) on a mica substrate, which is also a noble substrate, was reported to be ~ 1.5 nm.[11] This matches very well with the thickness of the adsorbed layer measured using the QCM-D in the present study, which also justifies the assumption of adsorbed layer density to be 1 g·cm^3. Moreover, based on the geometry of the molecule, the thickness of a perfectly vertically aligned layer of BDA-C14 molecules (Figure 1) on a flat surface is approximately 1.9 nm. Hence, at 1.5 nm, it can be reasonably assumed that the predominant configuration of inhibitor molecules for the QCM-D measured adsorbed layer is in some sort of a tilted configuration, which is again consistent with the results reported for BDA-C14 using AFM measurements and molecular simulations in separate studies.[11,21] Although to verify this conclusion, solely based on QCM-D measurements, more experiments are needed. Further studies will include testing this model inhibitor compound at different bulk inhibitor concentrations and also quantifying kinetics of adsorption/desorption.

CONCLUSIONS

The key takeaways from inhibitor adsorption experiments using QCM-D for the BDA-C14 model inhibitor compound are as follows:

i. Nature of the adsorbed layer: Elastic (rigid). More precisely, the adsorbed inhibitor layer behaves as a rigid mass as compared to ambient bulk solution.
ii. Sauerbrey's equation and SLA model were used to estimate the net mass absorbed and adsorbed layer thickness for BDA-C14 model inhibitor compound.
iii. At bulk inhibitor concentration of 100 ppm(w), QCM-D results match very well with the reported adsorbed layer thickness measured using AFM for the same BDA-C14 molecule on a mica substrate.

ACKNOWLEDGEMENTS

The author would like to thank the following companies for their financial support:
Ansys, Baker Hughes, Chevron Energy Technology, Clariant Corporation, ConocoPhillips, ExxonMobil, M-I SWACO (Schlumberger), Multi-Chem (Halliburton), Occidental Oil Company, Pertamina, Saudi Aramco, Shell Global Solutions, and Total Energies.

REFERENCES

1. M.G. Fontana, *Corrosion Engineering*, 3rd. ed. (Tata Mc Graw Hill Education Private Limited, 2005), p. 282.
2. V.S. Sastri, *Green Corrosion Inhibitors: Theory and Practice*, (John Wiley & Sons, Inc., 2011).
3. E. McCafferty, *Introduction to Corrosion Science*, (Springer New York, 2010), p. 357.
4. D. A. Jones, *Principles and Prevention of Corrosion*, (Prentice Hall International, 1996).
5. J.M.D. Olivo, B. Brown, & S. Nesic, "Modeling of corrosion mechanisms in the presence of quaternary ammonium chloride and imidazoline corrosion inhibitors," CORROSION 2016, paper no. 7406 (Vancouver, BC, Canada: NACE 2016).
6. J.M.D. Olivo, B. Brown, D. Young, & S. Nešić, "Electrochemical model of CO_2 corrosion in the presence of quaternary ammonium corrosion inhibitor model compounds," CORROSION 2019, paper no. 13392 (Nashville, TN: NACE 2019).
7. J.M.D. Olivo, "Electrochemical Model of Carbon Dioxide Corrosion in the Presence of Organic Corrosion Inhibitors," (Ph.D. Thesis: Ohio University, 2020).
8. M. Hepel, "Electrode-Solution Interface Studied with Electrochemical Quartz Crystal Nanobalance," *Interfacial Electrochemistry Theory: Experiment, and Applications*, (Taylor and Francis Group, 1999), p. 599–630.
9. M.C. Dixon, "Quartz crystal microbalance with dissipation monitoring: Enabling real-time characterization of biological materials and their interactions," *J. Biomol. Tech.* 19 (2008): pp. 151–158.
10. N. Moradighadi, et al., "Determining Critical Micelle Concentration of Organic Corrosion Inhibitors and its Effectiveness in Corrosion Mitigation," *Corrosion* 77, 3 (March 2021): pp. 266–275.
11. H. Wang, S. Sharma, A. Pailleret, B. Brown, & S. Nešić, "Investigation of Corrosion Inhibitor Adsorption on Mica and Mild Steel Using Electrochemical Atomic Force Microscopy and Molecular Simulations," *Corrosion* 78, 10 (October 2022): pp. 978–990.
12. K. Singla, H. Perrot, O. Sel, B. Brown, & S. Nesic, "Use of Quartz Crystal Microbalance in Study of Inhibitor Adsorption," CORROSION 2021, paper no. 16653 (Virtual Conference, Houston TX: 2021).
13. M.D. Hanwell, et al., "Avogadro: an advanced semantic chemical editor, visualization, and analysis platform," *J. Cheminform*. 4, 17 (2012).

14. Y.J. Montagut, et al., “Frequency-shift vs phase-shift characterization of in-liquid quartz crystal microbalance applications,” *Rev. Sci. Instrum.* 82, (2011): pp 064702-1 – 064702-14.
15. A.A. Vives, et al., “Method and Device for Nanogravimetry in Fluid Media Using Piezoelectric Resonators,” US patent 8869617B2 (2011).
16. G. Sauerbrey, “Verwendung von Schwingquarzen zur Wägung dünner Schichten und zur Mikrowägung,” *Zeitschrift für Phys.* 155 (1959): pp. 206–222.
17. D. Johannsmann, *The Quartz Crystal Microbalance in Soft Matter Research,* (Springer International Publishing, 2015), p. 143.
18. M. V. Voinova, M. Rodahl, M. Jonson, & B. Kasemo, “Viscoelastic Acoustic Response of Layered Polymer Films at Fluid-Solid Interfaces: Continuum Mechanics Approach,” *Phys. Scr.* 59 (1999): pp. 391-396.
19. D. Johannsmann, W. Bücking, B. Bode, & J. Petri, “Simple frequency-based sensing of viscosity and dielectric properties of a liquid using acoustic resonators,” *IEEE Trans. Ultrason. Ferroelectr. Freq. Control* 57 (2010): pp. 677–683.
20. D. Johannsmann, “Viscoelastic, mechanical, and dielectric measurements on complex samples with the quartz crystal microbalance,” *Phys. Chem. Chem. Phys.* 10 (2008): pp. 4516.
21. S. Sharma, H. Singh, & X. Ko, “A Quantitatively Accurate Theory To Predict Adsorbed Configurations of Linear Surfactants on Polar Surfaces,” *J. Phys. Chem. B* 123 (2019): pp. 7464–7470.